Synthesis of Novel ZnV$_2$O$_4$ Hierarchical Nanospheres and Their Applications as Electrochemical Supercapacitor and Hydrogen Storage Material

Faheem K. Butt,[†,⊥] Muhammad Tahir,[†] Chuanbao Cao,*[,†] Faryal Idrees,[†] R. Ahmed,[‡] Waheed S. Khan,[†] Zulfiqar Ali,[†] Nasir Mahmood,[§] M. Tanveer,[†] Asif Mahmood,[§] and Imran Aslam[†]

[†]Research Centre of Materials Science, Beijing Institute of Technology, Beijing 100081, People's Republic of China

[‡]Physics Department, Faculty of Science, Universiti Teknologi Malaysia, Skudai 81310 Johor, Malaysia

[§]Department of Materials Science and Engineering, Peking University, Beijing 100871, P.R. China

[⊥]Ibnu Sina Institute for Fundamental Science Studies, Universiti Teknologi Malaysia, 81310 Johor, Malaysia

Ⓢ *Supporting Information*

ABSTRACT: Hierarchical nanostructures (Hs) have recently garnered enormous attention due to their remarkable performances in catalysis, electronic devices, energy storage and conversion. Considering the advantage of hierarchical nanostructures, we have formulated a facile and template free method to synthesize novel hierarchical nanospheres (NHNs) of ZnV$_2$O$_4$. Both zinc and vanadium are earth abundant, relatively economical and can offer several oxidation states, which can render a broad range of redox reactions favorable for electrochemical energy storage applications. Keeping these points in mind, we investigated for the first time the electrochemical supercapacitor performance of NHNs. The electrochemical measurements were performed in 2 M KOH solution. The measured specific capacitance of ZnV$_2$O$_4$ electrode is 360 F/g at 1 A/g with good stability and retention capacity of 89% after 1000 cycles. Moreover, the hydrogen storage properties of NHNs were measured at 473, 573, and 623 K with an absorption of 1.76, 2.03, and 2.49 wt %. respectively. These studies pave the way to consider ZnV$_2$O$_4$ as prospective material for energy storage applications.

KEYWORDS: *ZnV$_2$O$_4$, hierarchical nanostructures, supercapacitor, energy storage, hydrogen storage*
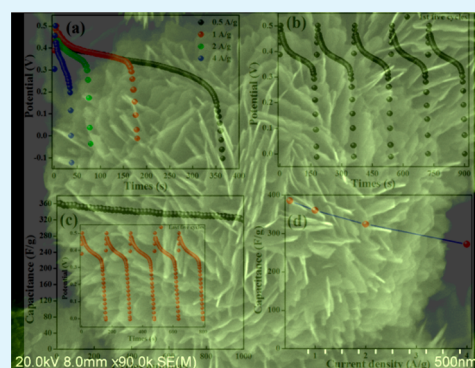
1. INTRODUCTION

As scaled-down consumer products appear on the horizon, there is a great need for energy storage in compact environments. Moreover, the ever increasing use of portable electronic devices such as cell phones, personal digital assistants (PDA), and laptops are swiftly exhausting traditional energy resources causing problems of environment pollution. These recent trends have trickled up the need for green and alternative renewable energy storage systems. Recently various substitutes are proposed as alternative of oil and fossil fuels such as lithium-ion batteries, supercapacitors, hydrogen storage materials and so forth.[1−3] Supercapacitors are a new class of storage devices that can bridge the gap between traditional dielectric capacitors and lithium-ion batteries. Supercapacitors are regarded as promising storage devices for use in portable devices, industrial power management, energy backups, electric vehicle, and so on. They proffer higher power densities with shorter charging time, longer operating life cycles, and better safety tolerance than batteries.[4−6]

On the other hand, considering environment safety, hydrogen is thought to be a promising alternative and sustainable green energy source. Although hydrogen storage has been given a great consideration for metal hydrides and metal organic frameworks (MOFs), less work has been reported for exploring the hydrogen-storage potential of nanostructured materials. However, considering the fact that nanomaterials can strongly influence the thermodynamics and kinetics of hydrogen absorption and dissociation, they can be promising hydrogen storage materials.

Generally, the performance of a supercapacitor is influenced by electrode material, type of electrolyte used and device assembly. Among these, the vital factor is electrode material. Hs which consist of nanosheets, nanorods, or nanoplates as primary substructures have demonstrated remarkable performances in energy storage, photochemical, photovoltaic solar cells, and other device applications.[7] Hs inherit advantages from primary substructures, whereas the secondary architectures in nanoscale regime provide superior stability, homogeneous porosity and resistance to aggregation. These features directly influence electrochemical performance. Among transition metal

oxides, vanadium-based oxides have shown promising pseudo-capacitance performance because of their high energy density, low cost, and copious resources.[8−10] However, synthesis of mixed transition metal oxides (MTrMO) of vanadium with hierarchical architectures still remains a great challenge. MTrMO could render rich redox reactions in electrochemical applications due to coupling of two metal species. Recently, ZnV_2O_4 spinel oxide has been proposed as promising material for energy storage applications such as lithium-ion batteries and hydrogen storage.[10,11] Various nanostructures of ZnV_2O_4 have been reported such as clewlike hollow structures, hollow spheres, nanosheets, and glomerulus nano/microspheres.[10−13] However, there exists no report on hierarchical nanostructures of ZnV_2O_4 as well as their applications in electrochemical supercapacitors.

Considering the advantages of MTrMO and hierarchical architectures, we have developed a facile method to fabricate the novel Hs of spinel ZnV_2O_4 for the first time. The NHNs were fabricated by a facile, template free and economical route. To elucidate the evolution of NHNs, time-dependent experiments were performed to propose the growth mechanism. The effect of precursor ratio and solvent were also studied. The synthesized NHNs are proposed for the first time as electrochemical supercapacitor electrode. The electrochemical supercapacitors exhibited good capacitance and retention capacity of 89% after 1000 cycles. The capacitance is higher as compared to other binary transition metal oxides pointing out the potential of NHNs as prospective materials for supercapacitor applications. Further, the enhanced hydrogen storage properties were exhibited by NHNs. These studies will pave the way for future earth abundant and economical electrochemical supercapacitors and energy storage materials.

2. EXPERIMENTAL SECTION

Sample Preparation. First, 0.24 g of NH_4VO_3 was added in 20 mL of methanol and sonicated. After a few minutes, $Zn(NO_3)_2$ was dissolved in the solution and vigorously stirred until a homogeneous solution was obtained. 0.5 g of Oxalic acid dehydrated $[H_2C_2O_4 \cdot 2H_2O]$ was added as a chelating agent afterward. Subsequently, equal volumes of H_2O_2 and HNO_3 were added dropwise into the solution. The resulting solution was transferred into a 50 mL of Teflon-lined autoclave, which was maintained at 200 °C for 24 h and then cooled to room temperature naturally. A black color product was obtained. These precipitates were collected and washed several times with absolute ethanol. Finally, the products were dried in a vacuum oven at 80 °C for 12 h.

Characterizations. The prepared product was characterized by X-ray diffraction (XRD) (Philips X'Pert Pro MPD with standard Cu−Kα radiation source, λ = 0.15418 nm). The morphological features were characterized by field emission scanning electron microscopy (FESEM), Transmission electron microscopy (TEM, JEOL-JEM-2100F), high resolution transmission electron microscopy (HRTEM) and selected area electron diffraction (SAED). The elemental composition was studied by energy dispersive X-ray spectroscopy (EDX). The chemical states were analyzed using X-ray photoelectron spectroscopy (XPS) using a PHI Quantera II (ULVAC-PHI, Japan) XPS System with monochromatic Al−Kα excitation under a vacuum better than 1×10^{-7} Pa.

Electrochemical Measurement. The ZnV_2O_4 NHNs 85%, activated carbon 10% and polytetrafluoroethylene (PTFE) 5% were mixed with ethanol, then pasted on nickel foam (5 cm × 1 cm) and dried at 80 °C for 24 h. Standard Calomel Electrode (saturated with KCl solution) and nickel foam were used as the counter and reference electrodes, respectively. The electrochemical behavior of the working electrode was analyzed in 2 M KOH in a three-electrode cell.

Hydrogen Storage Measurements. The hydrogen absorption of ZnV_2O_4 spinel oxide was measured by an isovolumetric method, using a commercial Sieverts type pressure−composition−temperature (PCT Pro-2000) apparatus. Three-tenths of a gram of the sample was loaded into a stainless steel container. The reactor was heated with an air furnace. All measurements were performed under a controlled vacuum atmosphere.

3. RESULTS AND DISCUSSIONS

A field-emission scanning electron microscopy (FESEM, Hitachi S-4800) was used to study the morphological characterizations of NHNs. It can be seen in Figure 1a, b
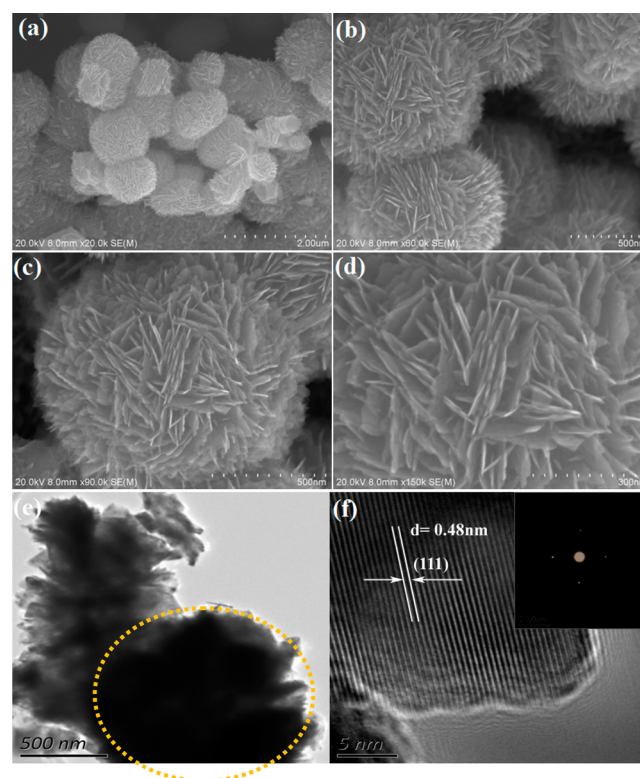
Figure 1. (a−d) FESEM images of ZnV_2O_4 hierarchical nanostructures. (e) TEM image of ZnV_2O_4. (f) HRTEM image of sample and the inset represents corresponding SAED pattern.

that the nanospheres are composed of primary substructures (nanosheet-like), which are the primary building blocks. Figure 1c, d shows the high-magnification image of hierarchical nanostrcutures. It was revealed that these spheres composed of very thin sheetlike structures around 10−15 nm on average. The secondary feature of nanosheets on primary structure of spheres provide additional capabilities as compared to ordinary nanostructures. A low-scale SEM image is provided in the Supporting Information, Figure S1. It shows large-scale synthesis of hierarchical nanospheres. Figure 1e shows TEM image of the hierarchical nanosphere. Figure 1f shows high-resolution TEM image (HRTEM) of the sample. The calculated interplanar distance was 0.48 nm, which corresponds to (111) plane of ZnV_2O_4 spinel structure.

The novel hierarchical nanostructures were further characterized by X-ray diffraction as shown in Figure 2a. The strongest peak was (311) at a position of θ = 35.395°. The lattice parameters were calculated to be a = b = c = 8.42 Å, which are consistent with standard value. All diffraction maxima

13636

dx.doi.org/10.1021/am503136h | ACS Appl. Mater. Interfaces 2014, 6, 13635−13641

Figure 2. (a) XRD pattern of ZnV_2O_4 NHNs. (b) Crystal structure of spinel ZnV_2O_4 with corresponding atoms. (c) EDX pattern of ZnV_2O_4 NHNs.

Figure 3. (a) Full scan of ZnV_2O_4 hierarchical nanospheres. High-resolution spectra of (b) V 2p, (c) Zn 2p, and (d) O1S peaks, respectively.

can be indexed with JCPDS no. 750318. No other secondary phases were observed indicating the pure phase of ZnV_2O_4. Figure 2b shows the interesting crystal geometry of spinel oxide ZnV_2O_4. It belongs to the FCC type crystal structure with $Fd\overline{3}m$ symmetry group. ZnO_4 tetrahedral and VO_6 octahedral building blocks form the crystal structure of ZnV_2O_4. The zinc atoms reside in the tetrahedral 8a position whereas the vanadium atoms are on 16d position, which forms a network of corner sharing tetrahedral structure. The oxygen atoms are at 32e position. The atomic composition of ZnV_2O_4 hierarchical nanostructures was analyzed by energy-dispersive X-ray spectroscopy affix with S-4800 FESEM. Zinc, vanadium and oxygen were the elements found by EDX analysis as shown in Figure 2c. No other atom/elements were detected indicating purity of the product. The atomic ratio was found to be 14.10:28.62:57.28, which are close to stoichiometric ratio of ZnV_2O_4.

To gain more insight about the purity of hierarchical nanospheres, we further analyzed the sample with the aid of XPS. Figure 3a illustrates the complete scan for detection of present elements in the sample. The V 2p XPS spectrum shown in Figure 3b presents further information for V 2p peaks at 515.77 and 523.15 eV. This indicates a V^{3+} state.[14] The spin orbit splitting, 7.38 eV, for the two peaks agrees well with the standard values.[13,14] The deconvolution of XPS peak of V 2p was carried out to observe the oxidation states of Vanadium explicitly. Another peak at position 517.2 and 524.8 eV, which belongs to V^{5+} state is also observed, which is due to surface oxidation or a little amount of V^{5+} state present in sample. The calculated atomic percentage of V^{5+} to V^{3+} state is only 8.2% of the sample. Figure 3c shows the Zn 2p spectrum. The previous studies indicate Zn $2p_{3/2}$ and Zn $2p_{1/2}$ peaks here belong to ZnV_2O_4.[13] The deconvoluted peaks of O 1s at 531.1 eV (Figure 3d) can be assigned to the adsorbed oxygen species such as OH, H_2O on the surface of ZnV_2O_4 hierarchical nanospheres.

To understand the growth mechanism for the hierarchical nanospheres, time dependent experiments were performed. The reaction after every 3 h of interval is shown in Figure 4a–f. It was observed that at 6 h reaction time, laminar-sheet like structures were formed as shown in Figure 4b. The agglomeration of laminar structure begins at 9 h as shown in Figure 4c. Increasing the reaction time to 12 h, the smaller sheet like structures aggregate to assemble themselves into clusters of nanosheets as shown in Figure 4d, e. It was further observed that the clusters of nanosheets begin to form roughly a spherical morphology. Increasing the reaction time to 18 h, it can be clearly seen that the nanosheets are self-assembled forming the hierarchical spherical nanostructures as shown in Figure 4f. The laminar-sheet like structures are self-aggregated to form spherical morphology in order to minimize the surface energy, which is favored thermodynamically. The time-dependent experiments and the evolution of morphology suggest that the formation of hierarchical nanospheres is due to Ostwald-ripening process.[15,16] The addition of a certain amount of $H_2C_2O_4 \cdot 2H_2O$ in the methanol solution of NH_4VO_3 and $Zn(NO_3)_2$ brings a yellowish golden color of the solution. This indicates that oxalate anions have performed the chelation of metal cations within the solution. Subsequent addition of HNO_3 and H_2O_2 give rise to dark brown color of the solution with an exothermic type reaction. In the presence of HCOOH in solution, the vanadium ion is reduced, giving a V^{3+} state and ZnV_2O_4 as a final product.[17]
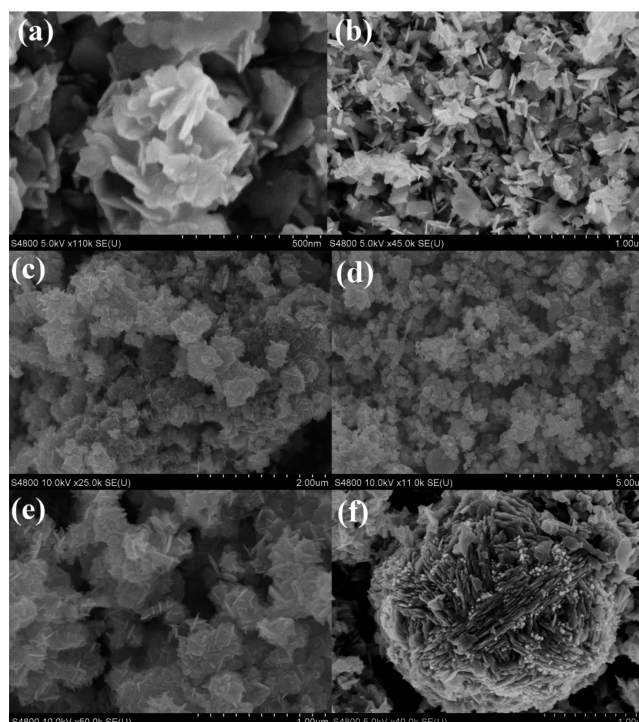
Figure 4. Time-dependent experiments for the growth of hierarchical nanospheres. Growth at (a) 3, (b) 6, (c) 9, (d)12, (e) 15, and (f) 18 h reaction time, respectively.

The role of reactants amount and the solvent was also studied further. A table in Supporting Information shows the different reaction schemes adopted to see the effect on morphology. The amount of reactants and the solvent was varied. It was observed that without the optimal conditions only irregular morphology was obtained. In case of scheme used in serial#1, irregular spherical shape morphology was observed as shown in Figure S2 in the Supporting Information. Some rodlike structures were seen in the case of scheme used in serial #2. Furthermore, it is pertinent to mention here that these schemes also do not lead to the pure phase of ZnV_2O_4. Therefore, we conclude that it is essential of maintaining a particular ratio of the reactants to obtain the hierarchical nanospheres of ZnV_2O_4. The role of solvent was observed by changing methanol with water while keeping other parameters constants. It can be seen in Figure S2 in the Supporting Information serial#3 that nanorodlike morphology is obtained.

Cyclic voltammetry (CV) was recorded in 2 M KOH aqueous solution within the potential range of 0 to 0.5 V. Figure 5(a) shows the CV curve of ZnV_2O_4 NHNs electrode at different scan rate (5, 10, 50, and 100 mV/s). The nonrectangular form of the CV curves is due to the pseudocapacitive contribution of ZnV_2O_4 NHNs. It also indicates that the capacity of ZnV_2O_4 NHNs electrode is due to the pseudocapacitive capacitance. It can also be seen that the capacitive behavior is maintained even at a high scan rate of 100 mV/s. There is one oxidation peak observed in the anodic process and one reduction peak observed in the cathodic process, which indicates that the capacitive characteristics are mainly governed by Faradaic reaction. The electrochemical measurements were executed in order to evaluate the supercapacitor performance of the ZnV_2O_4 NHNs in KOH electrolytes at current density of 0.5, 1, 2, and 4 A/g that are shown in Figure 5b. In Figure 5(b) first charging discharging
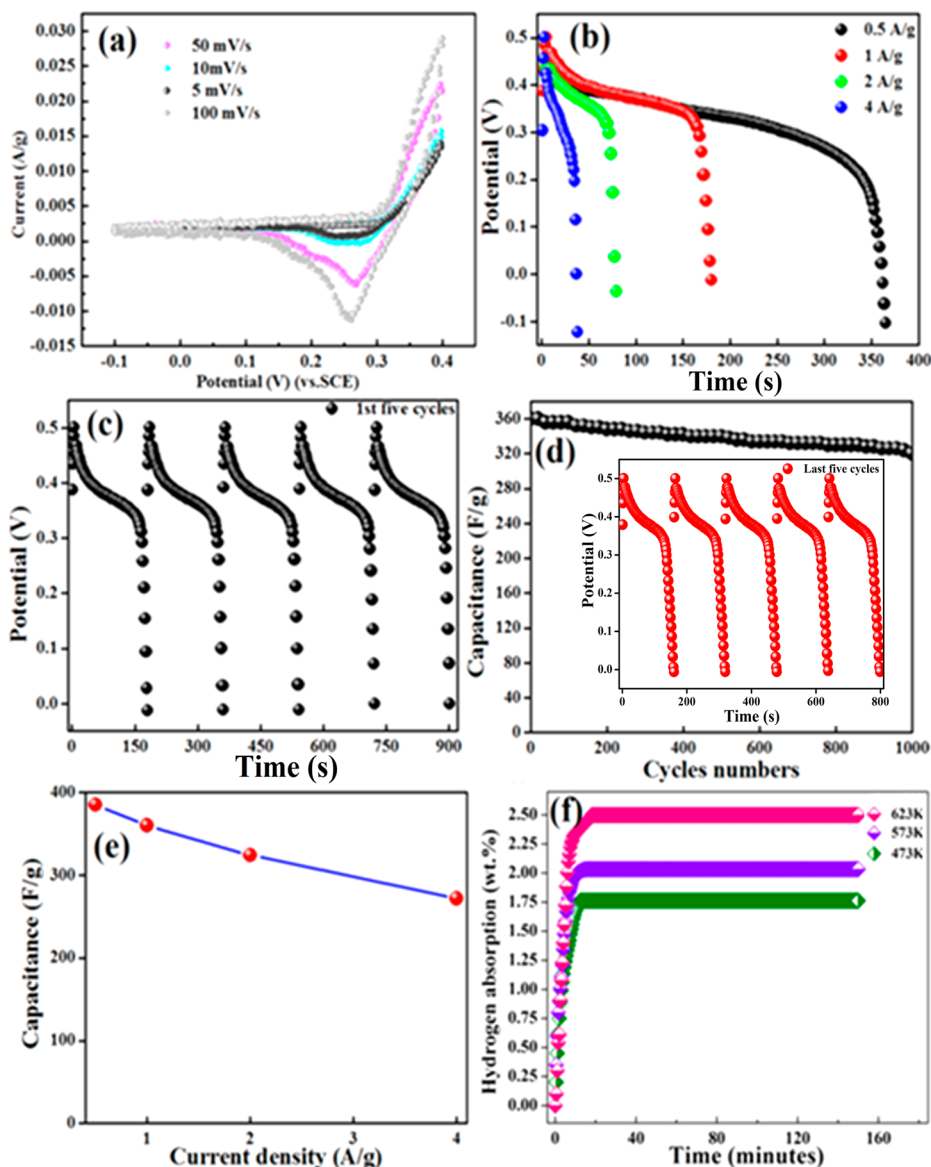
Figure 5. (a) CV of ZnV_2O_4 NHNs at different scan rates in 2 M KOH. (b) First charging–discharging curves of ZnV_2O_4 NHNs within a potential window of 0–0.5 V in 2 M KOH at different current density. (c) First five charging–discharging curves of ZnV_2O_4 NHNs within a potential window of 0–0.5 V in 2 M KOH at 1 A/g. (d) Cyclic performance of ZnV_2O_4 NHNs at 1 A/g (inset figure shows the last five charging discharging curve of ZnV_2O_4 at 1 A/g). (e) Capacitance as a function of current density. (f) Hydrogen absorption curve at different temperature.

cycle at different current density was shown. The time taken by first cycle at 0.5 A/g is almost doubling at taken by 1 A/g and the time taken by 4 A/g is much lower as can be seen in figure. Figure 5c shows the first five charge–discharge curves of ZnV_2O_4 NHNs electrode at current density of 1 A/g. The discharging time of all five cycles is same that shows good stability of ZnV_2O_4 NHNs as a supercapacitor electrode. It is believed that galvanostatic charge/discharge technique is a more accurate technique for measuring supercapacitance, so the specific capacitances (C) were calculated from galvanostatic charge/discharge curves according to the equation

$$C = \frac{(tI)}{(Vm)}$$

Where I is the current, t is the discharging time, m is the mass, and V is the voltage window of working electrode. The electrode composed of ZnV_2O_4 NHNs electrode shows specific

capacitance of 360 F/g at current density of 1 A/g for first cycle and 320 F/g for 1000th cycle that possess its good long-term cycling stability in KOH. This high value of supercapacitance is due to its unique structure of 3D nanospheres and growth of 2D nanosheets that assemble to make 3D nanospheres. The other possible reason is may be the combination of Zn and V make it very suitable for supercapacitance.[8,18] The inset of Figure 5d shows the last five charging discharging curve of ZnV_2O_4. Again the cyclic stability of ZnV_2O_4 NHNs can be seen very clearly as the discharging time of last five cycles is also not very different. The cycling performance is an important factor to determine the practical applications of an electrode material in real life. Furthermore, it proves excellent retention capability of 89%, such a good retention capability shows the structural stability of the ZnV_2O_4 NHNs electrode during electrochemical process.

Figure 5e shows specific capacitance of the ZnV_2O_4 NHNs electrode as a function of current density. The specific

capacitance of ZnV_2O_4 NHNs electrode is 385, 360, 324, and 272 F/g at current density of 0.5, 1, 2, and 4 A/g, respectively. From Figure 5e, it is obvious that the ZnV_2O_4 NHNs retains a good capacitance of 272 F/g at current density of 4 A/g, which confirms that the ZnV_2O_4 NHNs electrode can be used at high current density for practical application. As the current density increases, the specific capacitance decreases that is due to the limited diffusion of the active ions on the electrode surface because of fast charging. At high current density, all the micropores are not accessible to the electrolyte, therefore the relative capacitance is less compared to the capacitance at low current density.[19,20]

The value of specific capacitance of ZnV_2O_4 hierarchical nanospheres is found to be higher than other materials as indicated in Table 1. This indicates that ZnV_2O_4 hierarchical

Table 1. Comparison of Other Similar Binary Metal Oxides

serial no.	materials	electrolyte (molarity)	specific capacitance (F/g)	current density (A/g)	ref
1	$CuFe_2O_4$ hollow fibers	1 M KOH	28	0.5	18
2	Hierarchically Porous $CuFe_2O_4$ nanospheres	1 M KOH	289.5	0.6	8
3	$CuFe_2O_4$ thin films	1 M NaOH	5.7	0.3 $\mu A/cm^2$	21
4	nanostructured $CuCo_2O_4$	3 M KOH	338	1	22
5	$MnCo_2O_{4.5}$ hierarchical architectures	1 M KOH	118.8	1	23
6	ZnV_2O_4 hierarchical nanospheres	2 M KOH	385	0.5	our work
			360	1	

nanospheres can be low cost promising material for supercapacitor applications. Further the hydrogen storage properties of ZnV_2O_4 hierarchical nanospheres were measured using a commercial Sieverts type PCT Pro-2000 apparatus. At higher values of pressure, the ideal gas law was corrected using van der Waals equation for the volume of gas molecules[13]

$$\left(p + \frac{n^2 a}{V^2}\right)(V - nb) = nRT$$

The hydrogen storage properties were measured at three different temperatures. It can be seen in Figure 5f that the maximum hydrogen storage at 473 K was 1.76 wt %, 2.03 wt % at 573 K and 2.49 wt %. at 623 K. The hydrogen absorption is found higher than recently reported ZnV_2O_4 (1.74 wt %) nanosheets[11] and ZnV_2O_4 glomerulus nano/microspheres (2.165 wt %.).[13] The enhanced hydrogen storage properties of ZnV_2O_4 NHNs can be ascribed to its special hierarchical assembly. These studies open new possibilities to consider ZnV_2O_4 as an economical and prospective material for energy storage applications.

4. CONCLUSIONS

In conclusion, we have devised an efficient, facile and template free technique for the fabrication of NHNs of ZnV_2O_4. The advantageous properties associated with hierarchical architecture lead to excellent electrochemical properties such as high specific capacitance, rate capability and charge−discharge

stability of ZnV_2O_4 NHNs electrodes. Further, the enhanced hydrogen storage capabilities for the NHNs were also observed. These studies exhibit the use of ZnV_2O_4, a MTrMO, for energy storage applications. The unique hierarchical nanostructures of ZnV_2O_4 can be further extended to wide range of applications such as lithium-ion batteries, sensors, and various electronic devices.

■ ASSOCIATED CONTENT

⑤ Supporting Information

Different reaction schemes adopted to see the effect of precursors and solvent on the morphology. This material is available free of charge via the Internet at http://pubs.acs.org/.

■ AUTHOR INFORMATION

Corresponding Author

*E-mail: cbcao@bit.edu.cn. Tel: +86 10 68913792. Fax: +86 10 68912001.

Notes

The authors declare no competing financial interest.

■ ACKNOWLEDGMENTS

■ REFERENCES

(1) Hu, Y. H.; Zhang, L. Hydrogen Storage in Metal-Organic Frameworks. *Adv. Mater.* **2010**, *22*, E117−E130.

(2) Schlapbach, L.; Zuttel, A. Hydrogen-Storage Materials for Mobile Applications. *Nature* **2001**, *414*, 353−358.

(3) Sakintun, B.; Lamari-Darkrim, F.; Hirscher, M. Metal Hydride Materials for Solid Hydrogen Storage. A review. *Int. J. Hydrogen Energy* **2007**, *32*, 1121−1140.

(4) Liu, C.; Li, F.; Ma, L. P.; Cheng, H. M. Advanced Materials for Energy Storage. *Adv. Mater.* **2010**, *22*, E28−E62.

(5) Boukhalfa, S.; Evanoff, K.; Yushin, G. Atomic Layer Deposition of Vanadium Oxide on Carbon Nanotubes for High Power Supercapacitor Electrodes. *Energy Environ. Sci.* **2012**, *5*, 6872−6879.

(6) Zhang, C.; Yin, H.; Han, M.; Dai, Z.; Pang, H.; Zheng, Y.; Lan, Y. Q.; Bao, J.; Zhu, J. Two-Dimensional Tin Selenide Nanostructures for Flexible All-Solid-State Supercapacitors. *ACS Nano* **2014**, *8*, 3761−3770.

(7) Shi, Y.; Zhu, C.; Wang, L.; Zhao, C.; Li, W.; Fung, K. K.; Ma, T.; Hagfeldt, A.; Wang, Ning. Ultrarapid Sonochemical Synthesis of ZnO Hierarchical Structures: From Fundamental Research to High Efficiencies up to 6.42% for Quasi-Solid Dye-Sensitized Solar Cells. *Chem. Mater.* **2013**, *25*, 1000−1012.

(8) Zhu, M.; Meng, D.; Wang, C.; Diao, G. Facile Fabrication of Hierarchically Porous $CuFe_2O_4$ Nanospheres with Enhanced Capacitance Property. *ACS Appl. Mater. Interfaces* **2013**, *5*, 6030−6037.

(9) Zhu, J.; Cao, L.; Wu, Y.; Gong, Y.; Liu, Z.; Hoster, H. E.; Zhang, Y.; Zhang, S.; Yang, S.; Yan, Q.; Ajayan, P. M.; Vajtai, R. Building 3D Structures of Vanadium Pentoxide Nanosheets and Application as Electrodes in Supercapacitors. *Nano Lett.* **2013**, *13*, 5408−5413.

(10) Xiao, L.; Zhao, Y.; Yin, J.; Zhang, L. Clewlike ZnV_2O_4 Hollow Spheres: Nonaqueous Sol−Gel Synthesis, Formation Mechanism, and Lithium Storage Properties. *Chem.—Eur. J.* **2009**, *15*, 9442−9450.

(11) Butt, F. K.; Cao, C.; Ahmed, R.; Khan, W. S.; Cao, T.; Bidin, N.; Li, P.; Wan, Q.; Qu, X.; Tahir, M.; Idrees, F. Synthesis of Novel ZnV_2O_4 Spinel Oxide Nanosheets and their Hydrogen Storage Properties. *CrystEngComm.* **2014**, *16*, 894−899.

(12) Duan, F.; Dong, W.; Shi, D.; Chen, M. Template-Free Synthesis of ZnV_2O_4 Hollow Spheres and their Application for Organic Dye Removal. *Appl. Surf. Sci.* **2011**, *258*, 189−195.

(13) Butt, F. K.; Cao, C.; Wan, Q.; Li, P.; Idrees, F.; Tahir, M.; Khan, W. S.; Ali, Z.; Zapata, M. J. M; Safdar, M.; Qu, X. Synthesis, Evolution and Hydrogen Storage Properties of ZnV_2O_4 Glomerulus Nano/Microspheres: A Prospective Material for Energy Storage, Int. *J. Hydrogen Energy* **2014**, *39*, 7842−7851.

(14) Muilenbenger, G. E. *Handbook of X-ray Photoelectron Spectroscopy*; Perkin-Elmer: Eden Prarie, MN, 1979.

(15) Xu, J. S.; Zhu, Y. J. α-Fe_2O_3 Hierarchically Hollow Microspheres Self-Assembled with Nanosheets: Surfactant-Free Solvothermal Synthesis, Magnetic and Photocatalytic Properties. *CrystEngComm* **2011**, *13*, 5162−5169.

(16) Cao, C.-Y; Guo, W.; Cui, Z.-M; Song, W.-G; Cai, W. Microwave-Assisted Gas/Liquid Interfacial Synthesis of Flowerlike NiO Hollow Nanosphere Precursors and their Application as Supercapacitor Electrodes. *J. Mater. Chem.* **2011**, *21*, 3204−3209.

(17) Mao, L.-J; Liu, C.-Y; Li, J. Template-Free Synthesis of VO_x Hierarchical Hollow Spheres. *J. Mater. Chem.* **2008**, *18*, 1640−1643.

(18) Zhao, J.; Cheng, Y.; Yan, X.; Sun, D.; Zhu, F.; Xue, Q. Magnetic and Electrochemical Properties of $CuFe_2O_4$ Hollow Fibers Fabricated by Simple Electrospinning and Direct Annealing. *CrystEngComm* **2012**, *14*, 5879−5885.

(19) Tahir, M.; Cao, C.; Butt, F. K.; Idrees, F.; Mahmood, N.; Ali, Z.; Aslam, I.; Tanveer, M.; Rizwan, M.; Mahmood, T. Tubular Graphitic-C_3N_4: A Prospective Material for Energy Storage and Green Photocatalysis. *J. Mater. Chem. A* **2013**, *1*, 13949−3955.

(20) Tahir, M.; Cao, C.; Mahmood, N.; Butt, F. K.; Mahmood, A.; Idrees, F.; Hussain, S.; Tanveer, M.; Ali, Z.; Aslam, I. Multifunctional g-C_3N_4 Nanofibers: A Template-Free Fabrication and Enhanced Optical, Electrochemical, and Photocatalyst Properties. *ACS Appl. Mater. Interfaces* **2014**, *6*, 1258−1265.

(21) Ham, D.; Chang, J.; Pathan, S. H.; Kim, W. Y.; Mane, R. S.; Pawar, B. N.; Joo, O.-S; Chung, H.; Yoon, M.-Y; Han, S.-H. Electrochemical Capacitive Properties of Spray-Pyrolyzed Copper-Ferrite Thin Films. *Curr. Appl. Phys.* **2009**, *9*, S98−S100.

(22) Pendashteh, A.; Rahmanifar, M. S.; Kaner, R. B.; Mousavi, M. F. Facile Synthesis of Nanostructured $CuCo_2O_4$ as a Novel Electrode Material for High-Rate Supercapacitors. *Chem. Commun.* **2014**, *50*, 1972−1975.

(23) Li, W.; Xu, K.; Song, G.; Zhou, X.; Zou, R.; Yang, J.; Chen, Z.; Hu, J. Facile Synthesis of Porous $MnCo_2O_{4.5}$ Hierarchical Aarchitectures for High-Rate Supercapacitors. *CrystEngComm* **2014**, *16*, 2335−2339.